Early morphodynamics of the sudden formation of beaches during the 2021 volcanic eruption of La Palma

Nicolás Ferrer [a], Néstor Marrero-Rodríguez [a,b,*], Abel Sanromualdo-Collado [a], Juana Vegas [c], Leví García-Romero [a,b]

[a] *Grupo de Geografía Física y Medio Ambiente, Instituto de Oceanografía y Cambio Global (IOCAG), Universidad de Las Palmas de Gran Canaria (ULPGC), Spain*
[b] *Geoturvol Research Group, Departamento de Geografía e Historia, Facultad de Humanidades, Universidad de La Laguna, Spain*
[c] *Grupo de Investigación en Patrimonio y Geodiversidad, Instituto Geológico y Minero de España (IGME), Consejo Superior de Investigaciones Científicas (CSIC), Madrid, Spain*

ARTICLE INFO

ABSTRACT

On 19 September 2021, a new Strombolian monogenetic volcano erupted on the island of La Palma (Canary Islands, Spain). During the 12-week eruption, a succession of lava flows progressed down the west-central slopes, descended down the coastal cliffs and advanced over a narrow island shelf, filling it in the form of lava deltas. After the stabilization of the lava deltas, the formation of beach-like sedimentary bodies could be observed. This works aims to document the rhythms and formation dynamics of these beaches in the first months after their emergence using orthophotographic materials obtained using unmanned aerial vehicles (UAVs). These technologies have allowed analysis of the subaerial coastal evolution of the lava deltas between October 2021 and May 2022 through high-resolution digital images of approximately weekly frequency. The study includes analyses of the dichotomous evolution (emergences, disappearances, disintegrations and coalescences), short-term surface and shoreline variability (by rates of variation, Shoreline Change Envelope and Net Shoreline Movement indicators) and medium-term surface and shoreline trends (by linear regressions and End Point Rate indicators). The observations show that the formation of shoreline sedimentary bodies was sudden, within 24–48 h after stabilization of the lava fronts, and that most were subsequently long-lasting. Despite their durability, the dynamics after their appearance show high morphological mutability. The analysis of the maritime regime has allowed us to interpret these early, abnormally changing dynamics as initial states of morphodynamic disequilibrium and adjustments towards morphological stability and equilibrium with the physical environmental conditions.

1. Introduction

The volcanic eruption of 19 September 2021 on the island of La Palma (Canary Islands, Spain) generated the penetration of 'a'ā lava flows into the sea and the filling of the shallow Quaternary shelf on the western volcanic flank in the form of prograding lava fans. These types of morphologies have been referred to as lava deltas or lava-fed deltas in the international scientific literature (e.g. Moore et al., 1973; Furnes and Sturt, 1976; Lipman and Moore, 1996; Mattox and Mangan, 1997; Smellie et al., 2013; Rodriguez-Gonzalez et al., 2022) and have received other local names in the Canary Islands ('low islands' or 'fajanas') and the Macaronesian archipelagos ('fajãs'). Kauahikaua et al. (2003, pp. 63)

define them simply as all lava built beyond the preeruption coastline. They are therefore inherent to the emergence, growth and lateral expansion of volcanic islands (Skilling, 2002; Ramalho et al., 2013), and have been described and characterized for decades in places such as Hawaii (Moore et al., 1973; Lipman and Moore, 1996; Mattox and Mangan, 1997; Umino et al., 2006; Soule et al., 2022), Iceland (Eiríksson, 1990; Stevenson et al., 2012), Antarctica (Skilling, 2002), the Canary Islands (Furnes and Sturt, 1976; Klügel et al., 1999; Rodriguez-Gonzalez et al., 2022), the Azores (Mitchell et al., 2008) and the Mediterranean Sea (Bosman et al., 2014).

Lava deltas have attracted interest in the study of the interaction between lavas and marine or lake water masses during volcanic

* Corresponding author.
E-mail addresses: nicolas.fvg@ulpgc.es (N. Ferrer), nestor.marrero@ulpgc.es (N. Marrero-Rodríguez), abel.sanromualdo@ulpgc.es (A. Sanromualdo-Collado), j.vegas@igme.es (J. Vegas), levi.garcia@ulpgc.es (L. García-Romero).

eruptions (Lipman and Moore, 1996; Moore et al., 1973; Mattox and Mangan, 1997; Skilling, 2002; Ramalho et al., 2013; Soule et al., 2022). Aerial photographs and topographic tools have helped to study the rates and shapes of subaerial mass growth of lava deltas (e.g. Mattox et al., 1993; Umino et al., 2006), while bathymetric technologies have contributed to a more detailed understanding of the submarine configurations of lava flows that penetrate the ocean (e.g. Mitchell et al., 2008; Bosman et al., 2014).

The generation of vitric sands (hyaloclastites) and volcanic breccias on lava flows that reach the coastal waters, produces an abundance of fragmentary materials at the base of the lava deltas. To the point of generating underwater structures similar to Gilbert-type river deltas (Ramalho et al., 2013). The generation of fragmentary subaqueous structures in lava deltas has been reported since the early 20th century (Russell, 1902, in Fuller, 1931) and has been documented in detail by later authors (Moore et al., 1973; Mattox and Mangan, 1997; Skilling, 2002; Ramalho et al., 2013; Soule et al., 2022). At Kilauea Volcano (Hawaii), Mattox and Mangan (1997) described hydrovolcanic explosivity associated with the penetration of basaltic lavas into the ocean. Moore et al. (1973) also observed the fragmentation into sand and breccia of pahoehoe lavas penetrating the sea. From the Canary Islands, Furnes and Sturt (1976) analyzed the transitional structures between the subaerial part and the subaqueous base as a function of tidal conditions and the morphological and rheological characteristics of the lava flows. Smellie et al. (2013) recognized a massive subaerial unit overlying a chaotic subaqueous unit with an abundant mixture hyaloclastite and vesicular clinkers on the Antarctic coasts.

Associated with the formation of the lava deltas generated in the eruption of La Palma in 2021, a series of beach-type epiclastic accumulations emerged on the new coastline filling in the erosive inlets at the front of these deltas. The formation and early evolution of beaches during volcanic eruptions is a phenomenon that has received little attention in the literature, despite the importance of beaches as a social resource. It is mentioned by Anderson (1903) in his description of historical eruptions in the West Indies; by Isshiki (1964) with respect to the eruptions on the island of Miyake-jima; and by Siggerud (1972) in reference to the 1970 eruption on the island of Jan Mayen. Calvet et al. (2003) comment on it in relation to recent eruptions on the island of La Palma and Eiríksson (1990) highlights the erosion of the delta cliff front as the main precursor of the production of sandy sediments on the coast in Iceland. Moore et al. (1973) and Ramalho et al. (2013) also remark on the phenomenon of the formation of new volcanic black sand beaches on the delta flanks in oceanic islands.

It can be stated that, although the mechanisms associated with the penetration of lavas into the sea, as well as their resulting structures and shapes, are relatively well established (Moore et al., 1973; Mattox and Mangan, 1997; Skilling, 2002; Ramalho et al., 2013; Soule et al., 2022), the formation of new coastal beaches at lava delta fronts is a relatively poorly investigated phenomenon. Although some studies mention the formation of beaches associated with lava deltas (Anderson, 1903; Isshiki, 1964; Siggerud, 1972; Moore et al., 1973; Eiríksson, 1990; Calvet et al., 2003; Ramalho et al., 2013), no detailed monitoring of beaches generated in coastal environments of active volcanic islands has been carried out. Therefore, the aim of this paper is to document this phenomenon in detail by analyzing the formation times of beaches arising in the lava deltas of the Tajogaite volcano (La Palma, Spain, 2021). Moreover, their early subaerial dynamics in the first three to five months after the stabilization of the lava fronts are described.

2. Study area

The 2021 Tajogaite eruption took place on the island of La Palma, at the westernmost volcanically active end of the volcanic island chain of the Canary Islands. This archipelago lies in the northeastern Atlantic Ocean, at about 28° north latitude and 15° west longitude, forming an east-west subalignment of eight major islands on the African tectonic
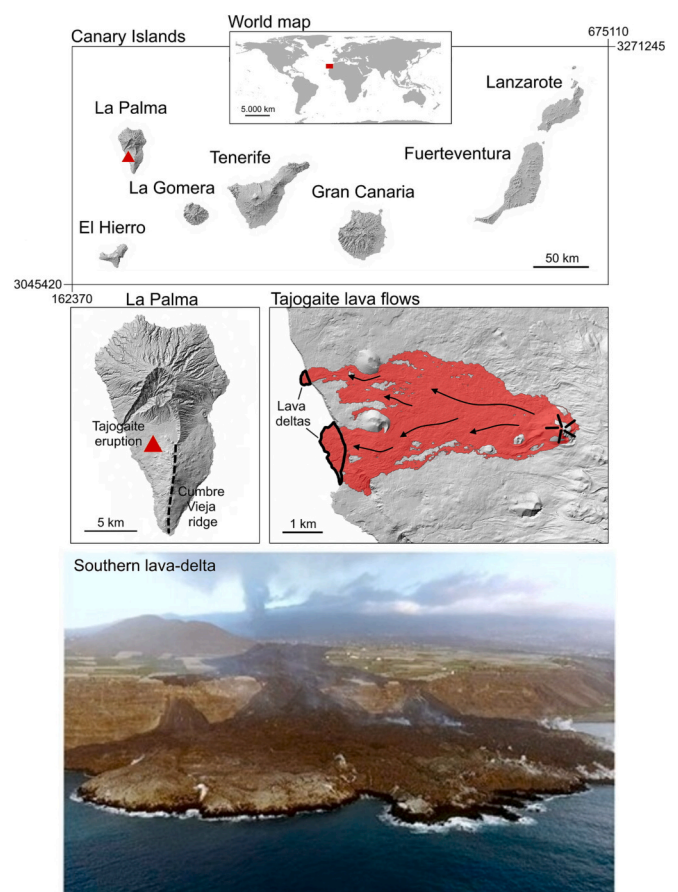
Fig. 1. Location of the Canary Islands, the island of La Palma and the eruptive complex of the Tajogaite volcano. The photo is from early October 2021, during the first growth phase of the southern delta.

plate (Fig. 1). Although evidence of a succession of ages (Lanzarote = 15.5 Ma, Fuerteventura = 20.6 Ma, Gran Canaria = 14.5 Ma, Tenerife = 7.5 Ma, La Gomera = 12.5, La Palma = 2.0 Ma, El Hierro = 1.1 Ma) has led to interpretation of the archipelago as a hotspot model (Wilson, 1963; Langenheim and Clague, 1987), with geophysical peculiarities that explain its "imperfect" spatio-temporal arrangement and long survival periods (Carracedo et al., 1998, 2001; Schmincke and Sumita, 1998; Carracedo, 1999; Acosta et al., 2005), the formation model and development of the Canary Islands is still under debate (Anguita and Hernán, 2000; Blanco-Montenegro et al., 2018).

The Tajogaite volcanic complex occupies an area of 12,250,000 m^2 in the central-western sector of the island of La Palma, northwest of the Cumbre Vieja volcanic ridge. Cumbre Vieja is a north-south rift formed during the Upper Pleistocene and Holocene (Carracedo et al., 2001; Acosta et al., 2005; Hoernle and Carracedo, 2009). With seven historical eruptions (Hernandez-Pacheco and Valls, 1982), it is considered the most active volcanic area in the Canary Islands. The eruption of the Tajogaite volcano was the product of a Strombolian-style monogenetic activity, typical in oceanic islands (Carracedo and Troll, 2016), with abundant pyroclastic emissions and fluid lava flows, mostly of type 'a'ā. More than 150 million cubic meters of lava were emitted from the eruptive vents (Civico et al., 2022) and flowed downslope until reaching the western coast. The lava flows plunged down the coastal cliffs and advanced along an island shelf (500 m wide and 25 m deep in average), forming two 'a'ā lava deltas backed by fossilized coastal escarpments (Fig. 1). The southern delta is the larger and formed in two events of lava flow penetration into the sea. The first occurred between 29 September and 9 October 2021, and the second between 13 November and 18 November 2021. It has an area reclaimed from the sea of 420,227 m^2

Table 1

Orthophotos used for the evolutionary study of the new beaches in the lava deltas of the Tajogaite volcano, indicating the oceanographic conditions (tide and swell) at the time the image was taken according from SIMAR point 4006017 (Spanish State Ports).

Ortophotos					Tidal and wave conditions			
Date	Time	Resolution (cm)	Vehicle	Measuring error (%)	Tide (cm)	Hs (m)	Tp (s)	Direction (quadr.)
29/09/2021	12.00	80.0	Drone[a]	4.76	−14.7	1.65	13.3	NW
29/09/2021	18.00	25.0	Drone[a]	0.88	17.0	1.55	13.3	NW
09/10/2021	18.00	25.0	Drone[a]	1.37	15.9	1.56	12.1	NW
10/10/2021	15.00	25.0	Drone[a]	1.04	83.1	1.13	11.0	NW
11/10/2021	12.00	25.0	Drone[a]	1.14	−45.8	1.04	16.1	NW
18/10/2021	11.30	15.0	Drone[a]	1.48	90.8	0.76	9.10	NW
25/10/2021	10.30	15.0	Drone[a]	0.88	−42.3	1.45	16.1	NW
01/11/2021	09.30	50.0	Drone[a]	1.66	64.5	1.46	12.1	NW
10/11/2021	12.30	20.0	Drone[a]	1.26	−44.4	0.84	14.7	NW
13/11/2021	11.00	30.0	Drone[a]	1.12	40.6	1.16	13.3	NW
18/11/2021	11.00	20.0	Drone[a]	0.75	60.4	1.16	13.3	NW
20/11/2021	10.00	25.0	Drone[a]	0.48	−19.2	0.85	12.1	NW
24/11/2021	10.15	20.0	Drone[a]	0.88	−43.2	1.14	10.0	NW
26/11/2021	10.00	25.0	Drone[a]	0.85	−18.5	0.63	9.10	SW
01/12/2021	10.30	15.0	Drone[a]	1.02	79.3	0.70	11.0	SW
07/12/2021	10.30	15.0	Drone[a]	1.03	−78.8	0.88	13.3	NW
08/12/2021	09.20	20.0	Drone[a]	2.32	−75.4	1.32	14.7	NW
12/12/2021	09.00	20.0	Drone[a]	0.86	53.7	1.57	16.1	NW
15/12/2021	11.00	25.0	Drone[a]	0.59	61.4	2.10	13.3	NW
14/01/2022	12.00	50.0	Satellite[b]	1.58	35.7	1.07	13.3	NW
01/03/2022	–	12.5	Aircraft[c]	1.45	–	–	–	–
06/05/2022	–	16.0	Aircraft[c]	–	–	–	–	–

[a] Orthoimage property of the La Palma Island Council and developed by TICOM SOLUCIONES S.L.
[b] Orthoimage property of the Government of the Canary Islands and developed by GRAFCAN S.A. from Airbus DS GEO Pleiades images.
[c] Orthoimage property of the Government of the Canary Islands and developed by GRAFCAN S.A.

and a subaerial volume of 9,391,854 m^3. The northern delta is notably smaller and formed from a single event between 23 and 24 November 2021. It has an area reclaimed from the sea of 48,556 m^2 and a subaerial volume of 552,424 m^3. The two deltas are part of a volcanic complex with a high geoheritage value in the context of the geology of the Canary Islands (Dóniz-Páez et al., 2022; Ferrer et al., 2023) and is included in the Spanish Inventory of Geosites.

3. Methodology

The identification and monitoring of the formation phases of the lava deltas and the new beaches were carried out by observing a time series of digital orthophotos taken during the eruption, between October and December 2021, and after the eruption, between January and May 2022. The 2021 orthophotographic series comes from the photogrammetric restitution of aerial images obtained on board unmanned aerial vehicles (UAVs) and is available for consultation on the open access data platform of the La Palma Island Council (https://www.opendatalapalma.es/) through the Web Map Service protocol (WMS). It consists of 50 orthophotos, 20 of which were selected to delineate the subaerial contours of the deltas, in their different phases of growth, and of the beach surfaces originating from the new coastline (Table 1). For analytic purposes, the images were grouped into low tides and high tides according to the tidal moment. The average frequency from the selected series is approximately weekly and the average spatial resolution is ~25 cm pix^{-1}. The 2022 orthoimages come from satellite platforms and manned photogrammetric flights with average resolutions of ~25 cm pix^{-1}, and are available for open consultation in the Spatial Data Infrastructure of the Canary Islands Government (https://www.idecanarias.es/) via WMS protocol (Table 1). Delimitation of the delta and beach contours was carried out by photo-interpretation in a GIS delineation environment, at a constant scale of 1:500, under a double criterion. First, by taking the water-land boundary, or perimeter of the flooded area; and then, by taking the dry beach boundary, or perimeter of the wet sand.

The study covered only the subaerial beach and does not include information from the submarine part of the system. The joint observation of the growth phases of the lava deltas and of the new beaches made it possible to delimit their emergence timing. Their subsequent evolution was studied by means of dichotomous, variability and trend analyses. The dichotomous analysis includes the identification of beaches and their temporal evolution in terms of maintenances, disappearances, disintegrations or coalescences. The short-time variability analysis reports the magnitude of beach surface growth or decline and the magnitude of shoreline advance or recession in terms of normalised relative rates (V$_{s\%}$) and absolute indicators (Shoreline Change Envelope and Net Shoreline Movement). The trend analysis of shorelines and beach surfaces provides an overall short- and medium-term evolutionary perspective using linear regressions and End Point Rate values with DSAS v5.0 software (Himmelstoss et al., 2018), using transects every 10 m and mean positioning uncertainties of 5 m at mean high water (MHW).

To ensure the comparative reliability of the measurements between orthophotos, longitudinal deviations were calculated with respect to the May 2022 orthophoto, whose planimetric error is higher than 0.62 m and lower than 1 m (GRAFCAN S.A., Government of the Canary Islands). The average deviation of the planimetric lengths, taking 10 ground control points not altered by the eruption, ranged from 4.76 % (in the orthophoto of 29/07/2021 at 12.00 h) to 0.48 % (in the orthophoto of 20/11/2021 at 10.00 h), with an overall standard deviation of 0.89 % (Table 1). The deviation values are much lower than the planimetric error of the May 2022 reference image (62–100 cm) and the resolution of the orthophoto series (12.5–80 cm), allowing confident comparisons to be made.

The swell analysis covers the period from 29 September 2021 to 6 February 2022. The raw data came from the Spanish State Ports SIMAR point 4006017 (Longitude: 18.00° W - Latitude: 28.67° N), located in deep water 7.5 km NW of the nearest sector of the lava delta. The SIMAR stations are simulation or re-analysis points that provide hourly mean values of different wave parameters, obtained by the numerical modelling of direct measurements from oceanographic buoys. The variables analyzed were the daily mean and maximum significant height (Hs), the daily mean peak period (Tp) and the daily mean direction.
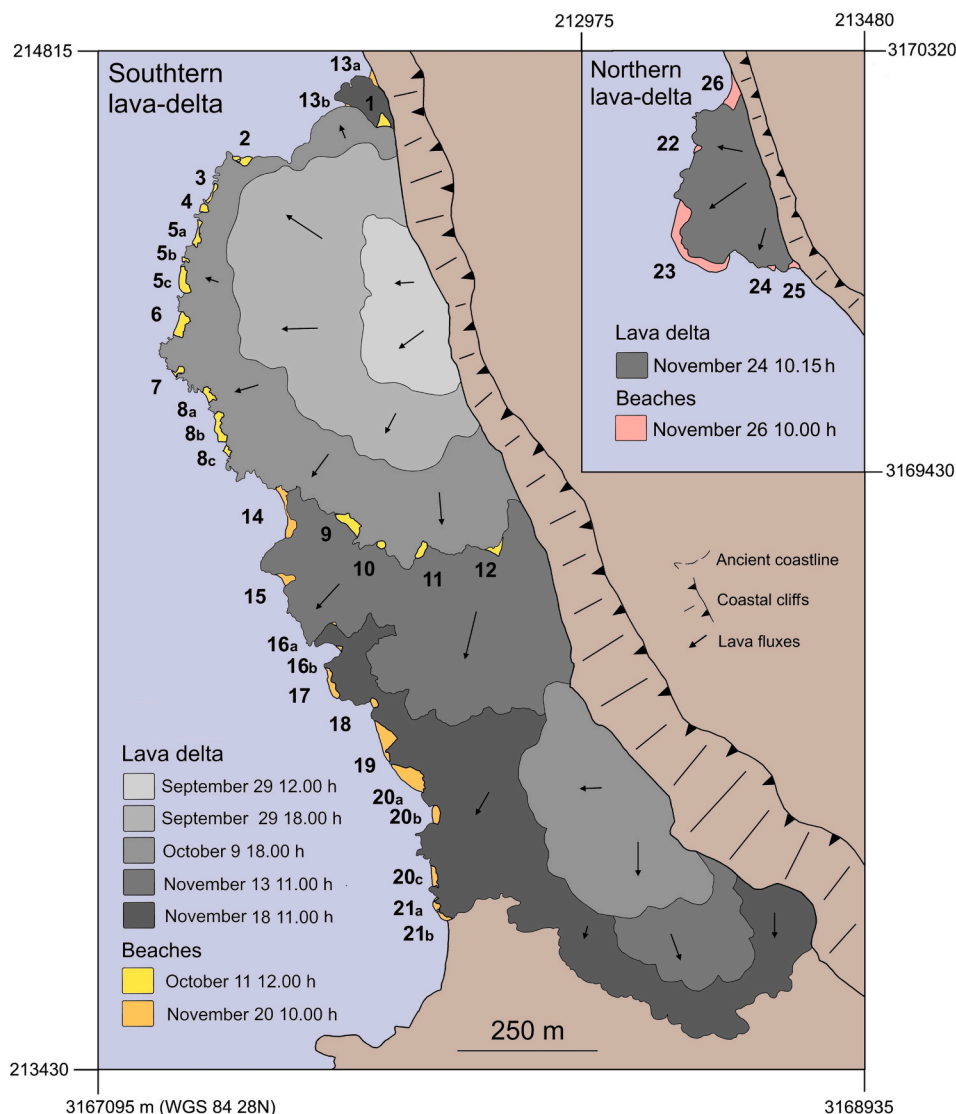
Fig. 2. Cartographic inventory of the delta formation phases of the Tajogaite volcano (La Palma, Canary Islands) and of the 34 beaches that emerged during the three events of the lava penetration into the sea.

4. Results

4.1. Emergence timing and beach census

Based on observation of the orthophotographic series, a total of 34 beach landforms suddenly emerged as a result of the penetration of Tajogaite volcano lava flows into the submarine shelf in three consecutive events. The final stabilization of the lava front during the first episode of construction of the southern delta occurred on 9 October 2021, and aerial photographs of 11 October, taken at 12 a.m. by cameras attached to a UAV, already reveal the appearance of 16 sedimentary deposits filling the rocky coast inlets. Therefore, <48 h elapsed from the time the lava front ceased its subaerial progradation along the platform until the incipient sedimentary beach bodies formed along the shores (Fig. 2, yellow). The second episode of construction of the southern delta started around 13 November 2021 and ended with the stoppage of the lava fronts on 18 November. This episode caused the delta to grow southwards, attaching to an earlier delta-type platform built from the superposition of historical eruptions on an older Pleistocene platform (Carracedo et al., 1994). As can be seen in the orthophotographic series, the growth of the delta towards the south, together with the advance of a small flow on the northern flank, buried 5 of the 16 beaches that had

developed during the first event of the formation of the southern delta, but produced, once again, the sudden formation of beaches on the new coastline. Thus, on 20 November at 10.00 a.m., approximately 48 h after the stabilization of the lava fronts, 13 beach deposits were again observed on the coastline (Fig. 2, orange). The third episode of delta formation took place on 24 November ~1 km north of the southern delta. This event produced the construction of a small lava fan of only 48,556 m^2 of emerged surface, where, for the third and last time, the sudden formation of 5 beaches could be observed after the stalling of the prograding lava front. Aerial images again reveal that the formation of the beaches occurred within a maximum lapse of 48 h, between 24 November at 10.15 a.m. and 26 November at 10.00 a.m. (Fig. 2, pink).

The beaches formed immediately after the three seaward penetration events were small in magnitude (Fig. 3). Beaches of the first event had a mean surface area between October and December 2021 of 608.1–646.8 m^2 (difference between high and low tides, respectively), with two orders of magnitude between the smallest beach (21.4–49.8 m^2) and the largest (2859.5-2244.7 m^2). Those of the second event had an average surface area (from November to December 2021) of 180.6–203.8 m^2, with two orders of magnitude between the smallest (180.6–203.8 m) and the largest beach (2510.1–2795.1 m^2); and those of the third event had an average surface area (from November to December 2021) of
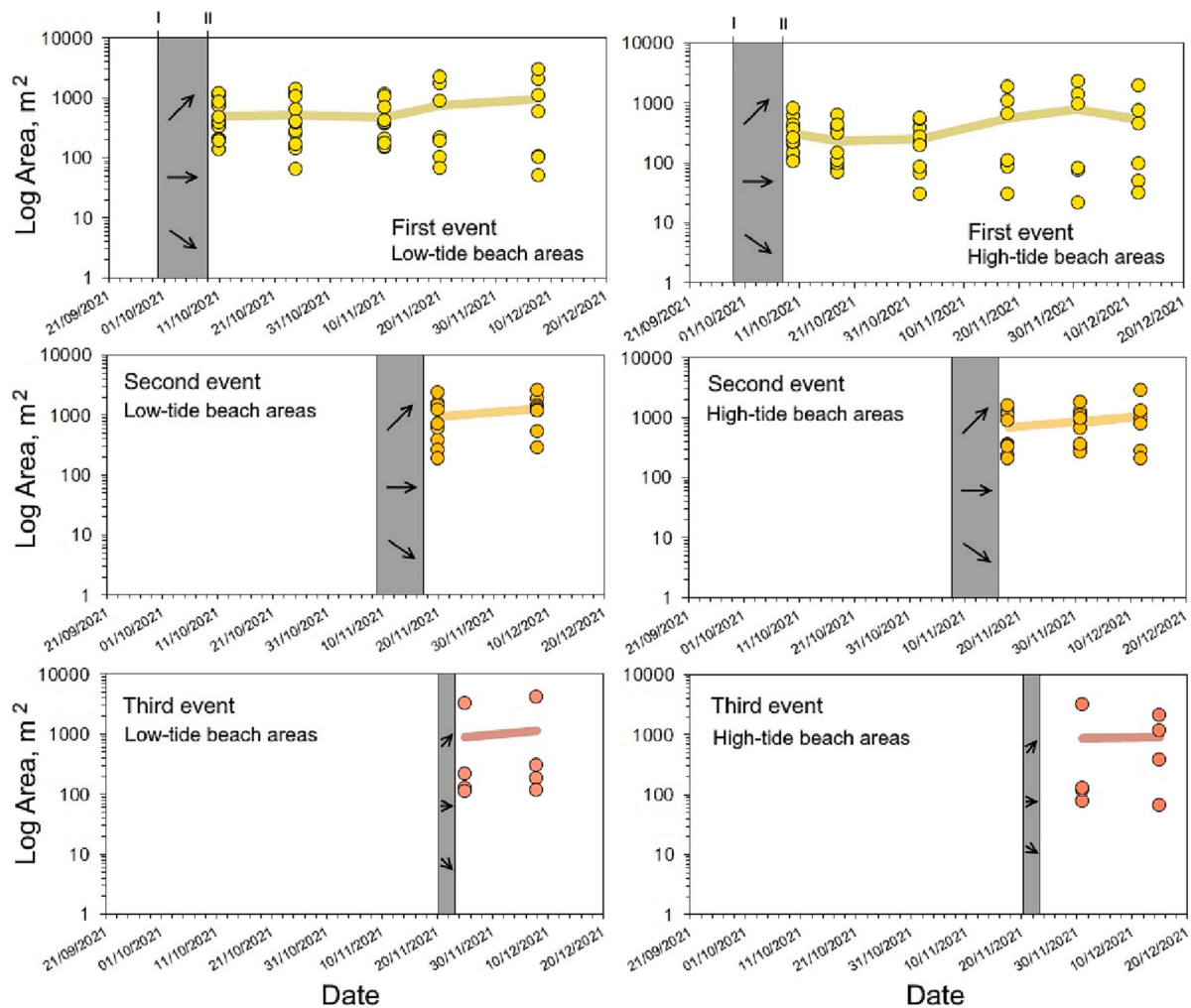
Fig. 3. Temporal relationship between the episodes of seaward lava intrusion (grey stripes) and the sudden beach emergence between September and December 2021, with the expression of their surface magnitude during the first months. From top to bottom, the three events; from left to right, the surfaces at low tide and high tide.

884.6–1029.4 m^2, with two orders of magnitude between the smallest (65.0–108.3 m^2) and the largest beach (3137.8-3998.0 m^2).

4.2. Maintenances, disappearances, coalescences and disaggregation

Once the beaches appeared suddenly (<48 h), they showed a high general durability throughout the time series of aerial images in the following months. Of the 16 beach deposits that appeared during the first event of the southern delta formation, only 2 could disappear due to dynamic causes (no. 7 and 12, Fig. 4), and 5 beaches were directly buried by the prograding lavas of the second event (no. 1, 9, 10 and 11, Fig. 4). With respect to the beach no. 12, may have disappeared due to the cumulative effect of Hs (significant wave height) >1.5 m during five days at the end of October and the beginning of November. And related to the beach no. 7, probably due to the storms of December, a month in which an average daily Hs of 2 m was exceeded on 48 % of the days and a maximum Hs of 4 m was reached on the 23rd and 24th days (Fig. 5). Similarly, of the 13 beaches that appeared after the end of the second constructive event in the southern delta, none disappeared in the following weeks and months, and, as an exception to the generally rapid appearance of beach bodies, a new deposit was formed more than two weeks after the front stopped (no. 16b, Fig. 4). The suddenly formed beaches in the northern delta were maintained during the following weeks and months, with the exception of the beach no. 24 (Fig. 4), which probably disappeared due to causes related to the Atlantic swells at the end of December 2021 (Fig. 5).

As could be detected through the weekly series of aerial images, most of the suddenly formed beaches persisted, albeit with significant short-term changes, mainly in the form of coalescence and disintegration between them (Fig. 4). Aggregation was the main evolutionary feature during the weeks and months following their appearance. A total of 6 beach deposits, out of the 16 identified in the first 48 h during the first construction event of the southern delta, had merged with others beaches two months later. Thus, beaches 5a-5b-5c merged into beach 5 and beaches 8a-8b-8c into beach 8. Likewise, of the 13 beaches suddenly formed after the second episode of lava prograding in the southern delta, 9 underwent coalescent evolutions in the following weeks and months, so that beaches 13a-13b merged into one, as did beaches 16a-16b, 20a-20b-20c and 21a-21b (Fig. 4). By early May 2022, approximately 5 months after the end of the Tajogaite volcano eruption, 80 % (n = 27) of the beach accumulations formed suddenly in the various events of lavas entering the sea had persisted. In this sense, 52 % of those cases had done so individually or aggregated into larger beach entities (these latter cases in 48 % of those cases). Of the beaches that disappeared (n = 7), only 3 could have been by erosional dynamics, while the remaining 4 were directly buried by the arrival of later lava flows (Fig. 4).
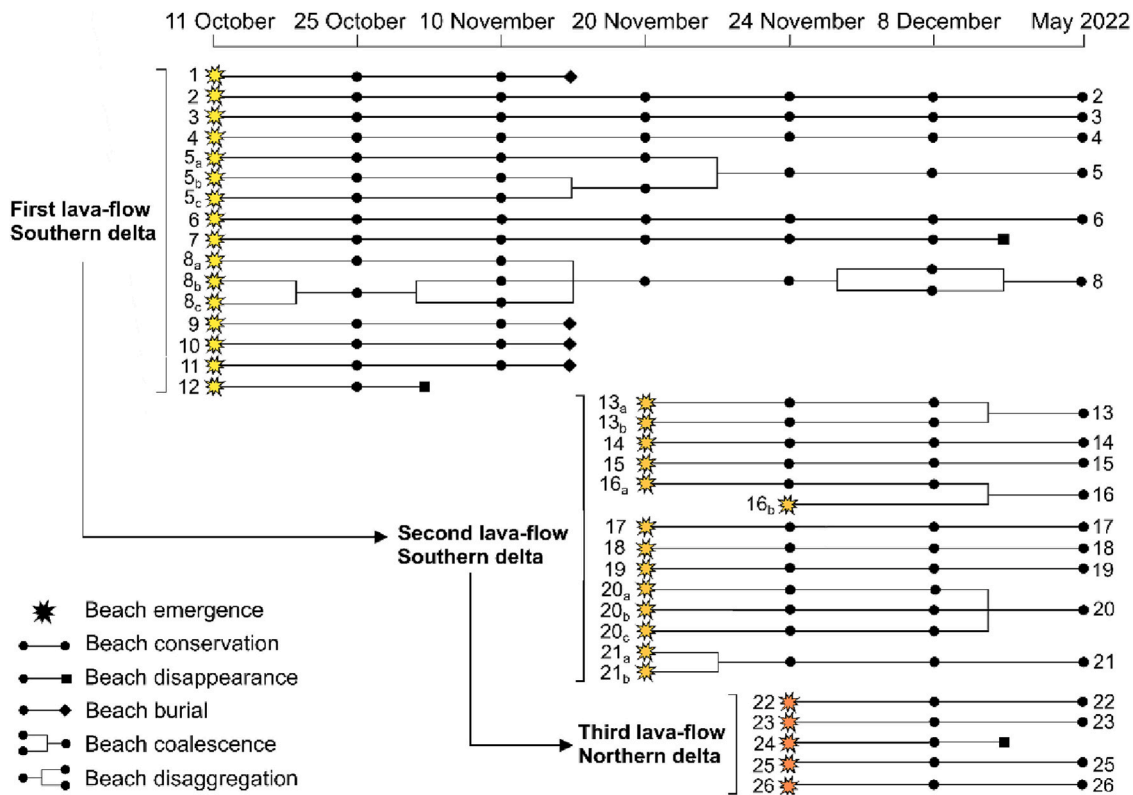
Fig. 4. Evolution between October 2021 and May 2022 of the 34 beaches that emerged in the different construction phases of the lava deltas of the Tajogaite eruption (island of La Palma, Canary Islands), in dichotomy terms: emergences, disappearances, coalescences and disaggregation.
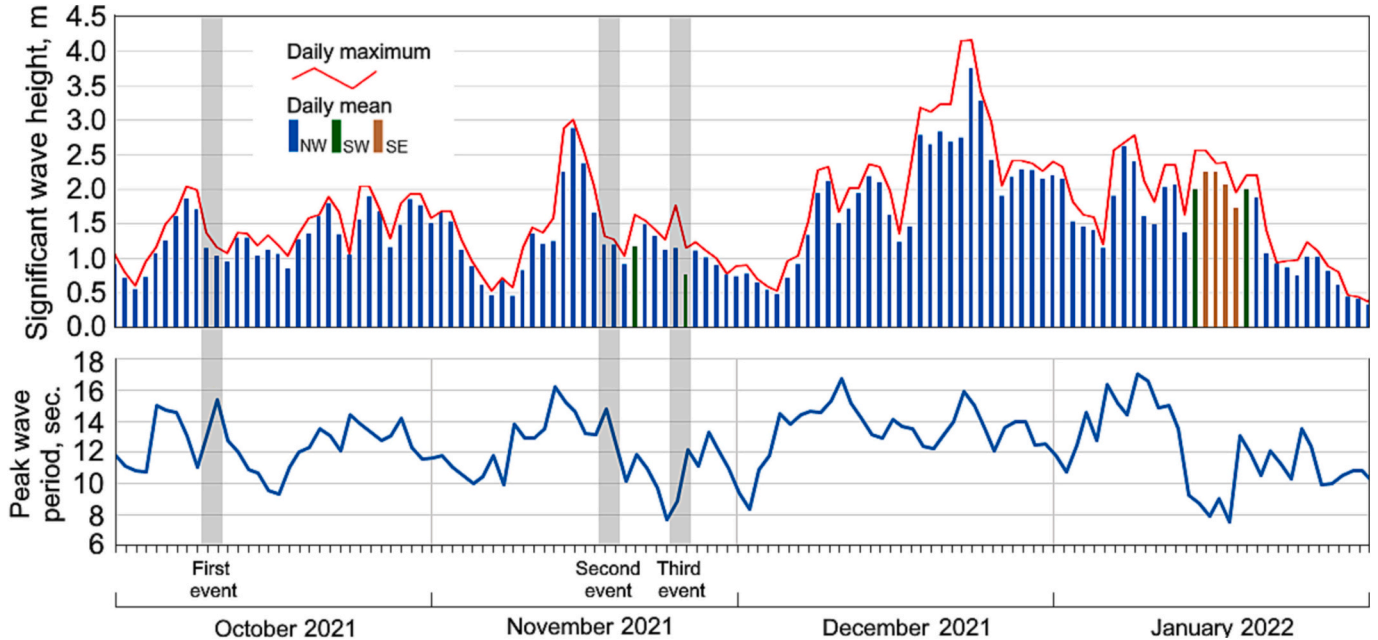
Fig. 5. Mean daily significant height, maximum daily significant height, peak period and mean swell direction, from October 2021 to January 2022, at SIMAR buoy 4006017, with indication of beach formation events (the width of the grey band marks the 48 h from stabilization of the lava front until beaches are observed).

4.3. Short-term surface variabilities in the eruptive period

The durability shown in the following months by the beaches of the Tajogaite lava deltas was marked by significant short-term morphological mutability (Fig. 6). The beaches formed during the first event in the southern delta maintained high surface dynamics between 10 October and 10 December 2021. Taking the dry beach observable limit as a reference, the surface variation rates ($V_{s\%}$) showed an absolute average ($|X|$) of 12.2 %, with a range from −75.2 % (beach 6) to 92.8 % (beach 8) and a general average of 10-day growth, except in the periods 10–20 October (−42.8 %) and 1–10 December (−32.1 %). Considering the land-water limit at low tide, $V_{s\%}$ showed a value $|X| = 17.7$ %, higher
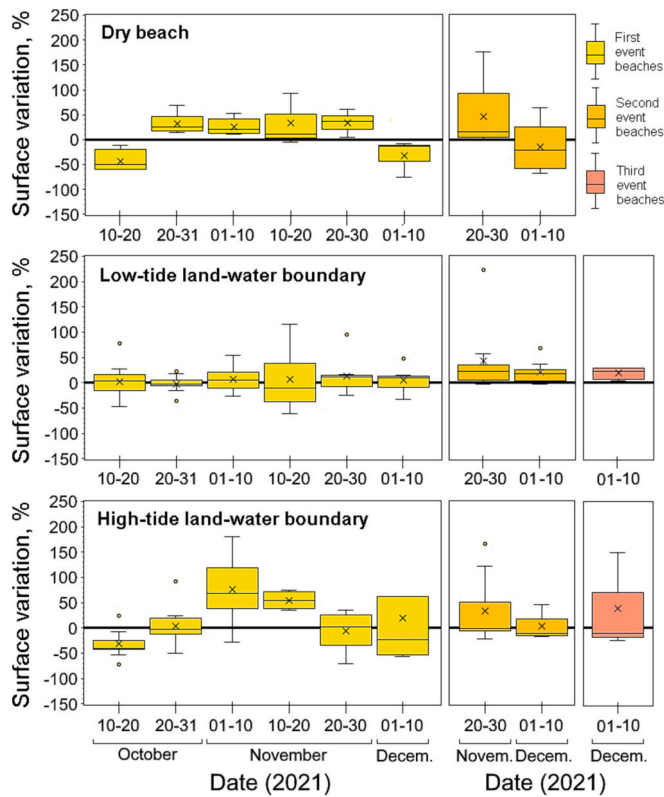
Fig. 6. Percentage variation, from October to December 2021, of beach surfaces, normalised to regular 10-day intervals, for the beaches of the first, second and third lava flow penetration events.

Table 2

Dynamics and trends of shorelines on Tajogaite lava delta beaches between October and December 2021, according to the indicators SCE = Shoreline Change Envelope (meters); NSM = Net Shoreline Movement (meters); EPR = End Point Rate (meters day^{-1}); EPR-UN = Uncertainty of End Point Rate (meters day^{-1}); LRR = Linear Regression Rate (meters day^{-1}); R2 = R-squared adjustment of the LRR estimate; LSE = Standard Error of the LRR estimate (meters); SS=Statistical Significance at confidence level, %.

ID	SCE	NSM	EPR	EPR-UN	LRR	R2	LSE	SS
1	12.89	−12.89	−1.61	0.88	–	–	–	–
2	5.59	−4.96	−0.11	0.17	−0.09	0.63	1.49	95.0
3	2.88	−2.88	−0.14	0.34	–	–	–	–
4	9.09	−9.09	−0.14	0.11	−0.13	0.84	1.92	90.0
5	7.22	−1.94	−0.11	0.28	0.06	0.25	4.12	90.0
6	10.86	1.04	0.02	0.13	0.11	0.34	4.16	90.0
7	4.86	−2.75	−0.03	0.33	−0.14	0.49	4.30	–
8	11.81	1.20	−0.03	0.15	0.06	0.52	3.80	95.0
9	4.63	2.10	0.12	0.36	0.09	0.20	3.16	–
10	5.14	4.59	0.26	0.36	0.14	0.73	1.11	–
11	6.91	6.91	0.30	0.31	0.36	0.95	1.34	90.0
12	8.64	0.20	0.01	0.31	0.08	0.08	6.34	–
13	2.03	−1.46	−0.07	0.35	−0.06	0.45	1.00	–
14	3.70	0.26	0.01	0.29	0.01	0.43	1.94	–
15	4.95	−4.87	−0.20	0.29	−0.19	0.90	0.81	95.0
16	3.10	−0.62	0.03	0.51	−0.21	0.86	0.83	–
17	15.67	−15.67	−0.65	0.29	−0.63	0.86	4.28	–
18	5.21	5.14	0.21	0.38	0.29	0.92	1.61	90.0
19	6.12	−5.51	−0.24	0.33	−0.25	0.76	1.84	–
20	5.27	−1.62	−0.08	0.35	−0.07	0.60	2.30	90.0
21	2.89	1.57	0.06	0.49	0.17	0.97	0.38	99.0
22	2.96	−2.96	−0.21	0.51	–	–	–	–
23	7.41	−6.88	−0.49	0.51	–	–	–	–
25	5.60	5.60	0.40	0.51	–	–	–	–
26	3.24	3.24	0.23	0.51	–	–	–	–

than under the previous observation criteria, with a range of −60.4 % (beach 7) to 115.3 % (beach 8) and an overall average 10-day growth, except in the period 20–31 October (−1.7 %, non-significant decrease). Taking into account the land-water boundary at high tide, $V_{s\%}$ showed a value $|X| = 27.2$ %, higher than under the two previous observation criteria, with a range of −71.3 % (beach 2) to 285.4 % (beach 3) and an overall average 10-day growth, except for the periods 10–20 October (−31.7 %) and 20–30 November (−5.3 %, non-significant decrease).

Beaches formed during the second event in the southern delta were even more dynamic than those of the first event during the same period (20 November to 10 December 2021). Taking the dry beach observable limit as a reference, $V_{s\%}$ showed a value $|X| = 27.9$ %, with a range from −68.2 % (beach 18) to 176.9 % (beach 16) and an increasing average rate for the period 20–30 November (47.0 %) and a decreasing one for the period 1–10 December (−14.3 %). In addition, the land-water boundary at low tide, $V_{s\%}$ showed a value $|X| = 24.6$ %, with a range of −2.2 % (beach 19) to 223.9 % (beach 16) and a significantly positive average variation for the period 20–30 November (40.7 %) and for the period 01–10 December (20.7 %). Looking also the land-water boundary at high tide, $V_{s\%}$ showed a value $|X| = 24.7$ %, with a range from −21.9 % (beach 19) to 166.1 % (beach 16) and a significant average growth for the period 20–30 November (33.3 %) and non-significant for the period 01–10 December (4.0 %). The beaches formed during the third event in the northern delta showed a similar dynamism to the beaches of the second event in the southern delta, for the same period (1–10 December 2021). Considering the land-water boundary at low tide, $V_{s\%}$ showed a value $|X| = 7.0$ %, with a range from 3.2 % (beach 24) to 28.8 % (beach 22) and a very positive overall average of 167.4 %; and with respect to the land-water boundary at high tide, $V_{s\%}$ showed a value $|X| = 66.8$ %, with a range from −23.6 % (beach 23) to 550.9 % (beach 26) and an average positive growth rate of 19.4 %.

The largest beach decreases, observed in the periods 1–10 October

and 1–10 December, cannot be clearly associated with the oceanographic conditions observed in the analysis of the wave series at SIMAR 4006017 (Fig. 5). In contrast, the generally increasing 10-day surface area variation is consistent with the overall observed conditions being low in energy and dominated by accretive swells. Between 10 October and 10 December, on only 11 days did the Hs value exceed 2 m at some time with NW swells, and on only one day did it reach 3 m.

Beach growths may be associated with widening of the backshore due to erosional retreat of the delta rock front rather than prograding shorelines on the beach faces. Between October and December 2021, the SCE indicator marked a mean of 6.3 m in absolute variation of shoreline positioning at MHW, with a maximum of 15.7 m (at beach 17) and a minimum of 2.0 m (at beach 13) (Table 2). According to the NSM and EPR indicators, the shoreline of the beaches had, between October and December 2021, both regressive (beaches 1, 2, 3, 4, 5, 7, 13, 15, 17, 19, 20, 22, 23) and prograding (beaches 6, 8, 9, 10, 11, 12, 14, 18, 21, 25, 26) trends. However, only on beaches 1, 4 and 17, was the uncertainty associated with the positioning lower than the EPR value itself. Linear regression rate (LRR) trends mostly coincided with trends in NSM and EPR, but showed an opposite sign (prograde) for beach 5. According to the LRR indicator, trends were significant at 90 % confidence for beaches 2, 4, 5, 6, 8, 11, 15, 18, 20 and 21, being higher than 95 % for beaches 2, 8, 15 and 21, and higher than 99 % for beach 21.

4.4. Mid-term tendencies from eruptive to post-eruptive period

Between October 2021 and May 2022, the surface evolution of the beaches also showed increasing and decreasing trends (Fig. 7). Five months after the end of the Tajogaite eruption, linear regressions revealed surface growth trends for beaches 2, 8, 13, 14, 16, 18, 20, 21, 23, 25 and 26, and decreasing trends for beaches 3, 4, 5, 6, 15, 17, 19 and 22. The highest growth was recorded at beach 21 (59.5 m^2 day^{-1}) and the highest decrease at beach 15 (−5.4 m^2 day^{-1}). The significance level of the ANOVA test for these regressions exceeded 90 % for beaches
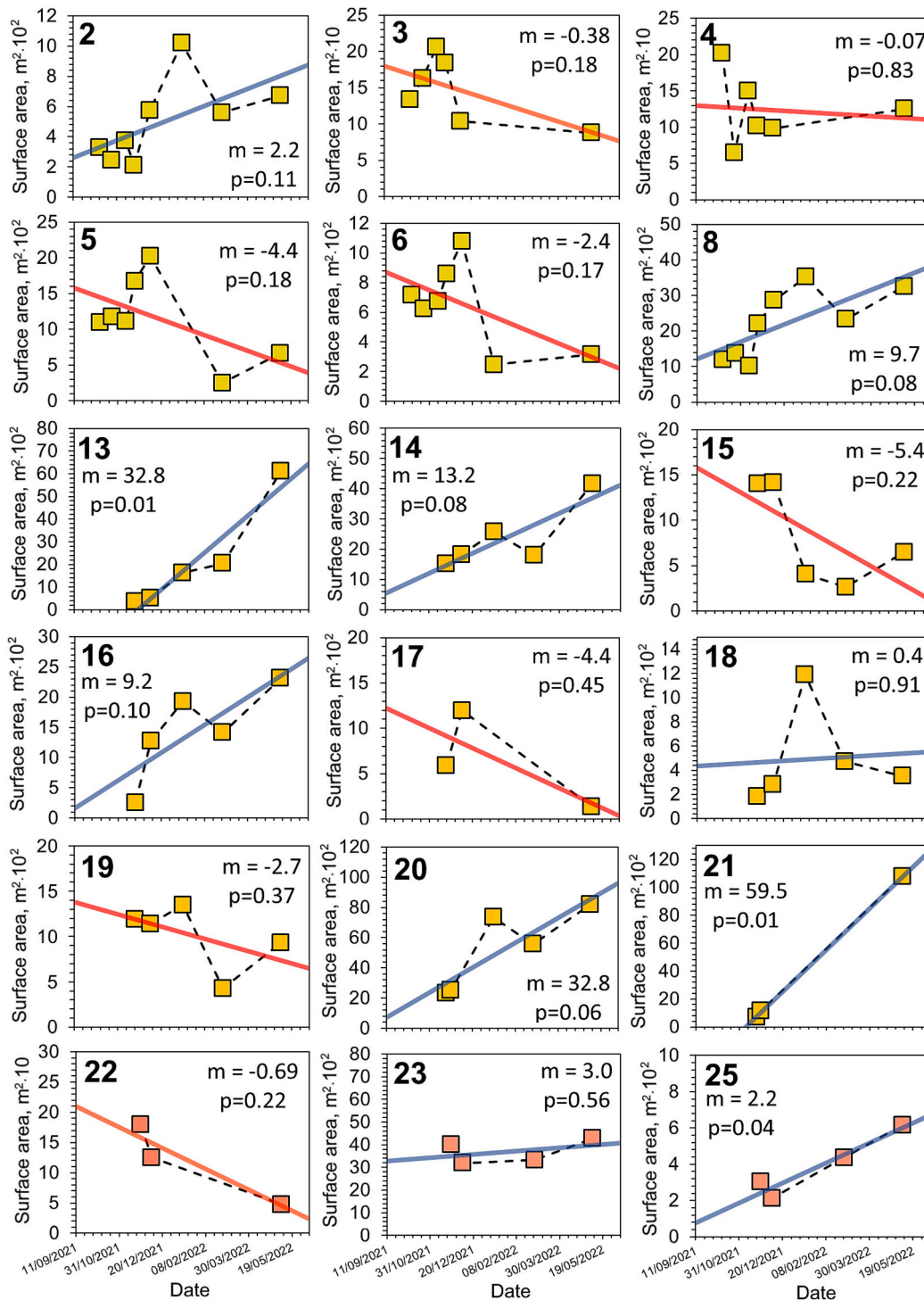
Fig. 7. Mid-term surface growth trends on Tajogaite lava delta beaches, estimated by linear regression, where slopes (*m*) are m² per day. The colours correspond to the three events of lava delta formation (first: yellow; second: orange; third: pink).

8, 13, 14, 16, 20, 21, 25 and 26 (all with positive surface growth), of which only beaches 13, 21, 25 and 26 reached a significance level of 95 %, and only beaches 13 and 26 exceeded a significance level of 99 %. In this same period, the shoreline experienced progradational trends on beaches 8, 13, 14, 20, 21 and 26, and regressive trends on beaches 2, 3, 4, 5, 6, 15, 16, 17, 18, 19, 22, 23 and 25; which were significant at the 95 % level on beach 8 and at the 99 % level on beaches 13, 14, 16, 20 and 21. The maximum progradation was recorded on beach 13 (0.14 m day⁻¹) and the maximum regression on beach 17 (−0.20 m day⁻¹). In five cases (beaches 2, 16, 18, 23 and 25) where the beach widening was

caused by the recession of the rocky foreshore front, the surface growth trend was accompanied by a regressive trend of the shoreline.

The distribution of these mid-term trends marks a north-south geographical pattern in both deltas (Fig. 8). In both the northern and southern deltas, medium-term beach growth has been maximum, and statistically significant, on the northern and southern flanks (beaches 13 and 21 in the southern delta and beaches 25 and 26 in the northern delta). Likewise, the negative growth and disappearance of beaches is concentrated in the central sectors of the lava deltas and, above all, in those most exposed to the dominant NW swells (beaches 3 to 7 in the
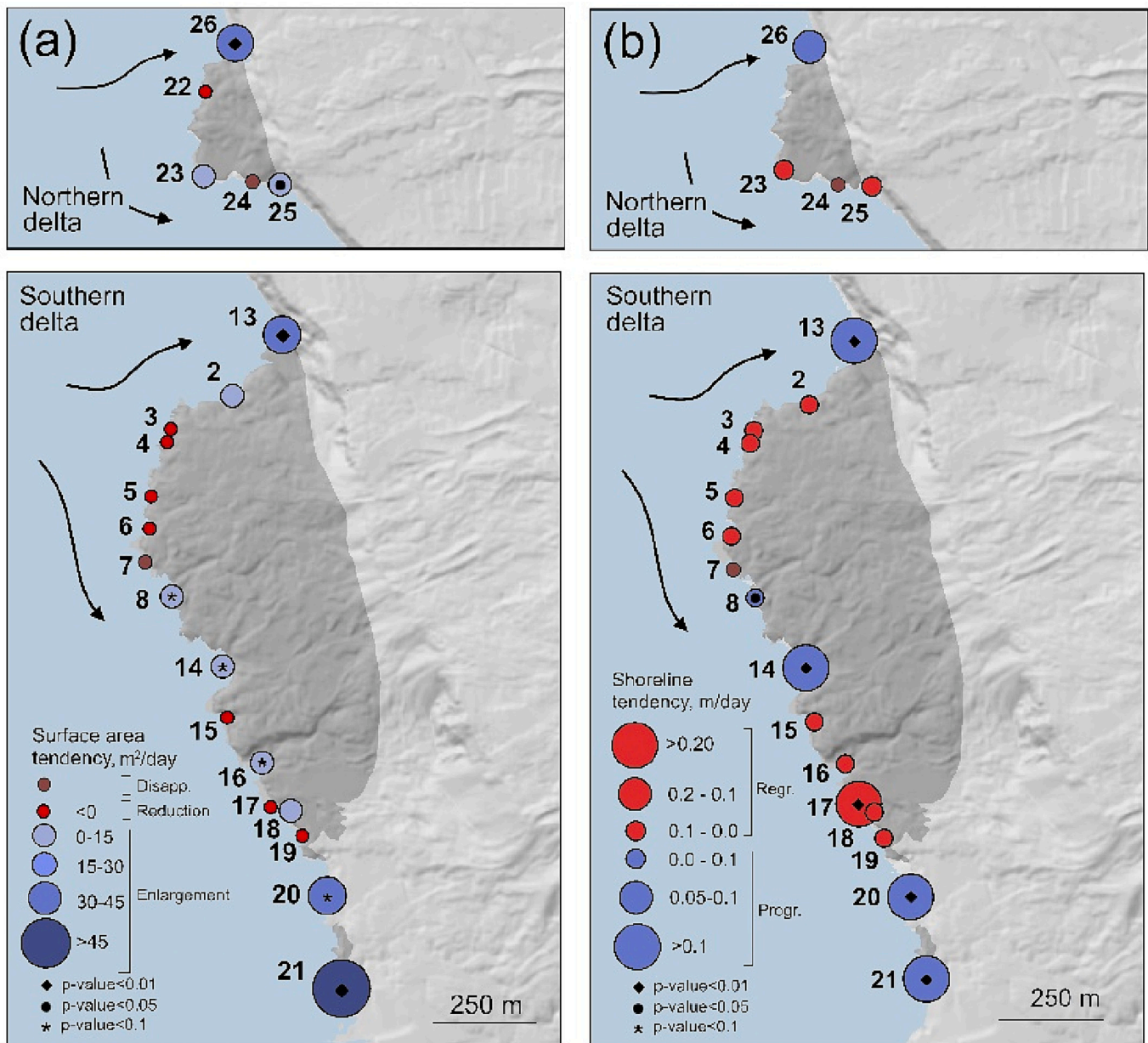
Fig. 8. Mid-term surface and shoreline trends on the beaches of the Tajogaite lava deltas. (A) Growth and decline trends of the surface of the beaches (m^2 day^{-1}). (B) Regression and progradation trends of the shoreline of the beaches (m day^{-1}).

southern delta and beach 22 in the northern delta). The period from 10 December to 2 January was the most energetic of the swell series analyzed (Fig. 5). Particularly between 19 and 26 December, when Hs values of 2 m were exceeded on eight consecutive days, and between 23 and 24 December, when over 4 m (Hs) swells from the NW occurred with peak periods of 16 s that could have significantly affected the NW-oriented beaches.

5. Discussion

The formation of beaches during volcanic eruptions has been referred to in works that dealt with near-shore eruptive processes (Anderson, 1903; Isshiki, 1964; Siggerud, 1972; Moore et al., 1973; Eiríksson, 1990; Calvet et al., 2003; Ramalho et al., 2013). In the Canary Islands, it was reflected, for example, in the chronicles of Don Juan Pinto of 17 January 1678 (Romero Ruiz, 1991), who describes how the great emission of 'sand' during the eruption of the San Antonio volcano

(island of La Palma) turned the rocky shores of the 'a'ā lava field into a sandy beach. This eruption in 1677 produced some similar morphologies to the Tajogaite deltas, and the presence of beaches can still be observed in several sectors. In fact, the presence of beaches in the shorelines of lava deltas is relatively frequent in the Canary Islands, in particular on the island of La Palma, where deltas are more abundant due to the high volcanic activity. About 37 % of the shore of La Palma is formed by lava deltas (Ferrer-Valero, 2018; Ferrer-Valero et al., 2019). Some 17 % of the coasts of these deltas are pebble and boulder beaches, and 8.5 % are sand and gravel beaches. The frequency of pebble beaches on the island of La Palma is higher outside deltas (44 %) than inside (17 %), but sand and gravel beaches are clearly more frequent on delta shores (8.5 %) than outside (4.9 %). These observations suggest that lava deltas may be relatively favorable coastal environments for the development of fine- and medium-grained beaches.

Although this fact has been acknowledged in the literature, until now there have been no data and images published on the early evolution of
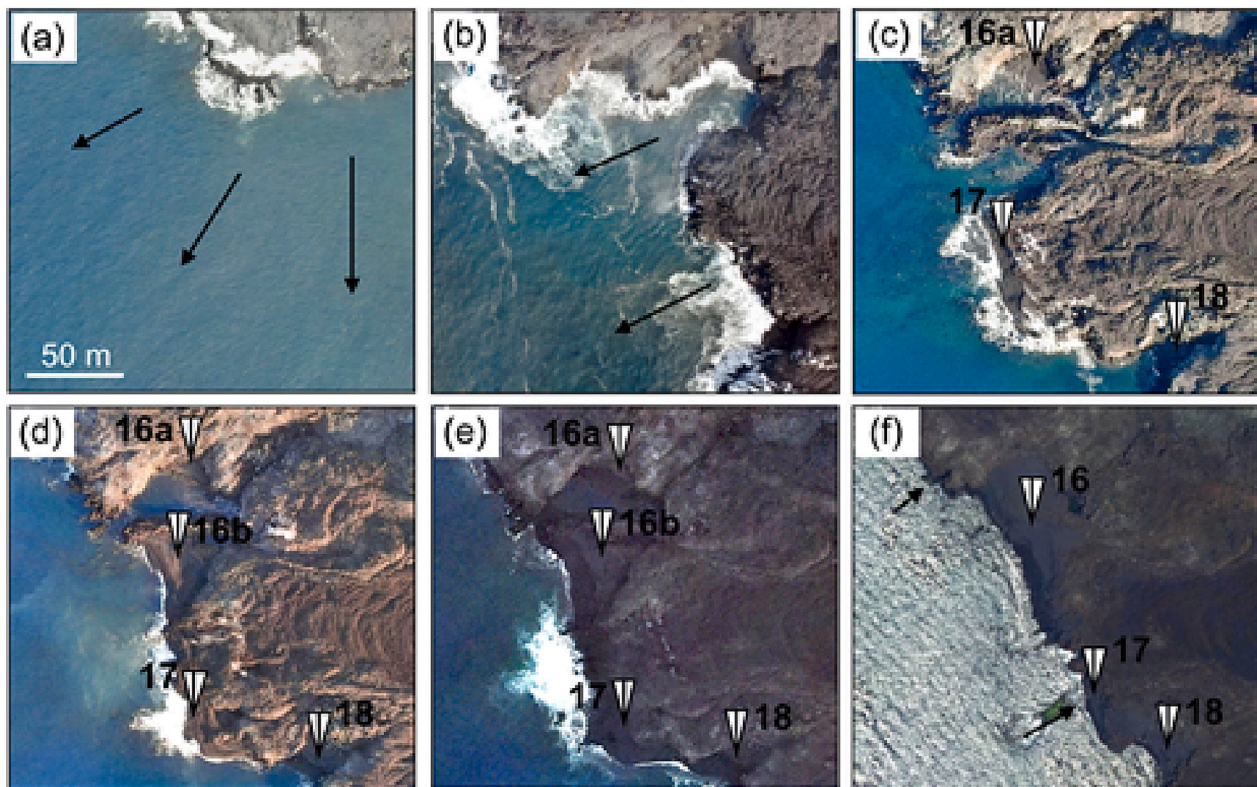
Fig. 9. Example of syn-volcanic beach formation and evolution in the southern delta of Tajogaite Volcano. (a) Beginning of the second penetration of lava flows into the sea on 11 November 2021; (b) the lava flows continue to advance on the island shelf on 15 November; (c) by 20 November the front has stabilized and beaches 16a, 17 and 18 appear; (d) on 1 December, beach 16b, which appeared a few days earlier, is observed; (e) on 1 December, a small lagoon is enclosed between beaches 16a and 16b, and the promontory where beach 17 develops begins to erode; (f) at the beginning of May 2022, beaches 16a and 16b have merged into one, beach 17 has receded by dozens of meters, losing part of its surface, and beach 18 persists by filling in a small inlet to the south.

beach formations during volcanic events. The Tajogaite eruption of 2021 has allowed us to document three consecutive episodes of lava flows penetrating the sea (Figs. 2 and 3), where the formation of coastal beaches occurred at intervals of <48 h, which is why we call this type of formation *syn-volcanic beaches* (simultaneous to the eruptive events). Sudden beach formation associated with the stabilization of a lava delta advance front can be associated with the rapid accumulation of fragmentary materials produced by the contact of lava flows with seawater. This penetration typically causes explosions with abundant production of glassy sands (hyaloclastites) and volcanic breccias at the shoreline and shoreface of the deltas (Moore et al., 1973; Furnes and Sturt, 1976; Mattox and Mangan, 1997; Skilling, 2002; Ramalho et al., 2013; Smellie et al., 2013; Soule et al., 2022). The rapid accumulation of these fragmentary materials by waves and currents could be the main mechanism for the rapid formation of beaches during the entering of lavas into the sea. However, the accumulation by waves and currents of ash and lapilli, deposited on the island shelf prior to the advances of the lava deltas could also have contributed significantly. The aerial emission of fragmentary lapilli and ash materials from the main eruptive centers of the Tajogaite volcano, ~5.5 km from the coast and ~1200 m asl, was very abundant between September and December 2021 and affected a radius of several kilometers (even reaching Tenerife, La Gomera and El Hierro). So the arrival of this type of material to the lava deltas of Tajogaite, and its re-deposition by waves on shoreline, could be expected.

The sudden appearance of these beaches during the eruptive event was followed by high mid-term durability and a general process of coalescence between beaches (Fig. 4, and see Fig. 9 for an example). In turn, the durability was accompanied by high morphological instability during the first weeks and months (Fig. 5). The beaches of the first event showed 10-day mean surface area variation rates of 19.0 %, with a maximum decrease of −75.2 % and a maximum growth of 285.4 %.

Those of the second event repeated a highly unstable behavior at 10 days, with average variation rates of 25.7 %, maximum decrease of −68.2 % and maximum growth of 223.9 %; and those of the third event were again highly changeable on a decadal scale, with average variation rates of 36.9 %, maximum decrease of −23.6 % and maximum growth of 550.9 %.

Rapid erosion of mature beaches, in equilibrium with the incident energy regime, is usually related to strong human disturbance of the shoreline (e.g. Saengsupavanich et al., 2008; Phillips, 2008a, 2008b; Marrero-Rodríguez et al., 2020, 2021) or storm surges (e.g. Harley et al., 2017; Cheng and Wang, 2019); circumstances that did not occur between mid-October and mid-December 2021 on the newly formed beaches in the Tajogaite volcano deltas. Therefore, it has not been possible to establish a particular relationship between the dynamics of surface decline and shore erosion and the daily wave conditions in the first two months, as these were generally low in energy (in fact, the main trend of the beaches in these first months was of progressive enlargement).

The great surface and shoreline variability can be interpreted that the *syn*-volcanic beaches, after a sudden appearance during the eruptive period, due to the accumulation of fragmentary volcanic material, were located outside morphodynamic equilibrium with the oceanographic conditions, showing a more sensitive behavior to small wave dynamics than the mature beaches. Thus, beach deposits formed suddenly would follow very unstable behaviors due, foreseeably, to a situation of strong morphological disequilibrium with the surrounding conditions. Such a differentiated behavior between the beaches of such a small coastal sector would support these observations. However, the inherent variability of short-term shoreline positioning, also on mature beaches (e.g. Smith and Zarillo, 1990; Harley et al., 2011), should be taken into account and these data should be treated with caution in view of the
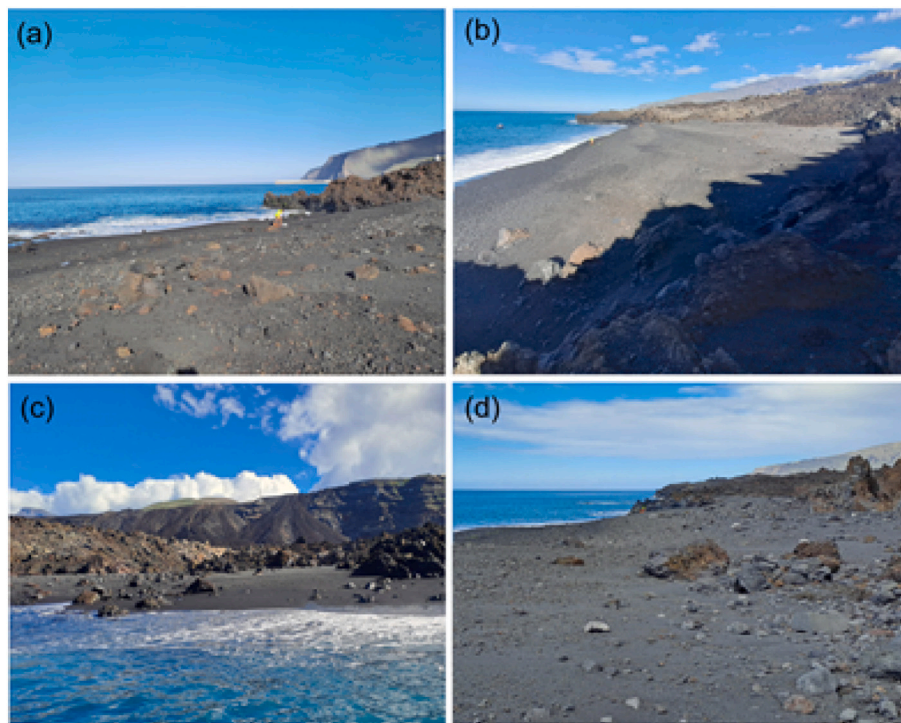
Fig. 10. Location of the main beaches of the Tajogaite lava delta in a field survey conducted on 15 January 2023, one year after the end of the eruption. Beaches have not yet received toponymy: (a) beach 23 from the inventory, ~4300 m²; (b) beach 14 from the inventory, ~4200 m²; (c) beach 16 from the inventory, ~2300 m²; (d) beach 20 from the inventory, ~8200 m². See Fig. 2 for locations.

positioning uncertainties linked to georeferencing, digitization and instantaneous tidal and wave conditions in orthophotos (Himmelstoss et al., 2018).

In the medium term, in the post-eruptive period, the beaches began to show patterns of growth/decline and erosion/accretion consistent with exposure to the dominant swell (Fig. 5). Indeed, the beaches with the highest NW exposure (beaches 3 to 7) showed clearly regressive surface losses and dynamics in the post-eruptive period, when the largest NW storms began to occur (Figs. 5 and 8). At the same time, the less exposed beaches, located on the flanks of the deltas, began to experience accretionary dynamics and surface enlargement, probably favored by sediment longshore transport from the erosional areas and the backshore widening (Fig. 8).

Despite the observed patterns, a more complete understanding of the morphodynamic behavior of the new beaches of Tajogaite will require a simultaneous examination of subaerial and subaqueous geomorphic transformations and structures. The Tajogaite volcano eruption significantly modified the marine shelf bathymetry introducing complex rocky structures that can determine wave breaking patterns, currents and sediment transport. Geological controls on coastal sedimentary dynamics are common worldwide (Trenhaile, 2016; Gallop et al., 2020). As in other many coasts (e.g., Muñoz-Pérez et al., 1999; Jackson et al., 2005; Gallop et al., 2012, 2013, 2020; Bosserelle et al., 2021; Rodríguez-Padilla et al., 2022), features such as rocky headlands and nearshore outcrops could largely control the sedimentary dynamics of the new beaches of Tajogaite at local scale and explain some of the differential beach behaviors.

In addition to the high short- and mid-term subaerial mutability of the Tajogaite syn-volcanic beaches, their emergence was marked by a sudden appearance (in hourly lapses) and high persistence, with only 3 out of 34 inventoried beaches disappearing completely, probably due to dynamic causes during the eruptive and post-eruptive periods. In a field visit to the beaches on 15 January 2023, approximately one year after the end of the Tajogaite eruption, the research team was able to verify in situ the significant development attained by some of these beaches of

syn-volcanic origin (Fig. 10). The appearance in a few hours and annual persistence of the Tajogaite beaches may raise new hypotheses about the origin of natural beaches and the timing of evolutionary models on volcanic coasts. When observing beaches that have been there for hundreds or thousands of years, it is difficult to think that their origin could have been so sudden, but the observations presented open up that possibility. We now believe that many other beaches in regions like the Canary Islands may have originated in this way.

In order to study their current equilibrium with the dynamic conditions and their behavior in the future, the research team is analyzing in detail the origin, shape and size of the sedimentary particles that make up the beaches, as well as their three-dimensional morphology, as part of a monitoring program that seeks to determine the stability and evolution of these beaches in the medium and long term. It is expected, for example, that the initial contributions of fragmentary volcanic material (hyaloclastites, breccia and tephra) will be joined by new contributions of carbonate marine sediments and sediments produced by long-term weathering processes of the rock escarpments of the deltaic fronts.

Declaration of competing interest

No conflict of interest exists.

Data availability

The authors are unable or have chosen not to specify which data has been used.

References

Acosta, J., Uchupi, E., Smith, D., Muñoz, A., Herranz, P., Palomo, C., ZEE Working Group, 2005. Comparison of volcanic rifts on La Palma and El Hierro, Canary Islands and the island of Hawaii. In: Geophysics of the Canary Islands: Results of Spain's Exclusive Economic Zone Program, pp. 59–90.

Anderson, T., 1903. Recent volcanic eruptions in the West Indies. Geogr. J. 21 (3), 265–279.

Anguita, F., Hernán, F., 2000. The Canary Islands origin: a unifying model. J. Volcanol. Geotherm. Res. 103 (1–4), 1–26.

Blanco-Montenegro, I., Montesinos, F.G., Arnoso, J., 2018. Aeromagnetic anomalies reveal the link between magmatism and tectonics during the early formation of the Canary Islands. Sci. Rep. 8 (1), 42.

Bosman, A., Casalbore, D., Romagnoli, C., Chiocci, F.L., 2014. Formation of an 'a'ā lava delta: insights from time-lapse multibeam bathymetry and direct observations during the Stromboli 2007 eruption. Bull. Volcanol. 76, 1–12.

Bosserelle, C., Gallop, S.L., Haigh, I.D., Pattiaratchi, C.B., 2021. The influence of reef topography on storm-driven sand flux. J. Mar. Sci. Eng. 9 (3), 272.

Calvet, F., Cabrera, M.C., Carracedo, J.C., Mangas, J., Pérez-Torrado, F.J., Recio, C., Travé, A., 2003. Beachrocks from the island of La Palma (Canary Islands, Spain). Mar. Geol. 197 (1–4), 75–93.

Carracedo, J.C., 1999. Growth, structure, instability and collapse of Canarian volcanoes and comparisons with Hawaiian volcanoes. J. Volcanol. Geotherm. Res. 94 (1–4), 1–19.

Carracedo, J.C., Troll, V.R., 2016. The Geology of the Canary Islands. Elsevier.

Carracedo J.C., Badiola R.E., Guillou H. (Dir. Cuaeto-Pascual L.A.) (1994). Mapa Geológico Nacional Hoja 1085III scale 1:25,000. Instituto Geológico y Minero de España, IGME, Madrid.

Carracedo, J.C., Day, S., Guillou, H., Badiola, E.R., Canas, J.A., Torrado, F.P., 1998. Hotspot volcanism close to a passive continental margin: the Canary Islands. Geol. Mag. 135 (5), 591–604.

Carracedo, J.C., Badiola, E.R., Guillou, H., de La Nuez, J., Torrado, F.P., 2001. Geology and volcanology of la Palma and el Hierro, western Canaries. Estudios Geologicos-Madrid 57, 175–273.

Cheng, J., Wang, P., 2019. Unusual beach changes induced by Hurricane Irma with a negative storm surge and poststorm recovery. J. Coast. Res. 35 (6), 1185–1199.

Civico, R., Ricci, T., Scarlato, P., Taddeucci, J., Andronico, D., Del Bello, E., Pérez, N.M., 2022. High-resolution digital surface model of the 2021 eruption deposit of Cumbre Vieja volcano, La Palma, Spain. Sci. Data 9 (1), 435.

Dóniz-Páez, J., Németh, K., Becerra-Ramírez, R., Hernández, W., Gosálvez, R.U., Escobar, E., González, E., 2022. Tajogaite 2021 Eruption (La Palma, Canary Islands, Spain): An Exceptional Volcanic Heritage to Develop Geotourism, 69. Proceedings.

Eiríksson, J., 1990. Clast shape development on a new lava beach at the Heimaey harbour, Iceland. J. Coast. Res. 486–506.

Ferrer, N., Vegas, J., Galindo, I., Lozano, G., 2023. A geoheritage valuation to prevent environmental degradation of a new volcanic landscape in the Canary Islands. In: Land Degradation & Development.

Ferrer-Valero, N., 2018. Measuring geomorphological diversity on coastal environments: a new approach to geodiversity. Geomorphology 318, 217–229.

Ferrer-Valero, N., Hernández-Calvento, L., Hernández-Cordero, A.I., 2019. Insights of long-term geomorphological evolution of coastal landscapes in hot-spot oceanic islands. Earth Surf. Process. Landf. 44 (2), 565–580.

Fuller, R.E., 1931. The aqueous chilling of basaltic lava on the Columbia River Plateau. Am. J. Sci. 5 (124), 281–300.

Furnes, H., Sturt, B.A., 1976. Beach/shallow marine hyaloclastite deposits and their geological significance: an example from Gran Canaria. J. Geol. 84 (4), 439–453.

Gallop, S.L., Bosserelle, C., Eliot, I., Pattiaratchi, C.B., 2012. The influence of limestone reefs on storm erosion and recovery of a perched beach. Cont. Shelf Res. 47, 16–27.

Gallop, S.L., Bosserelle, C., Eliot, I., Pattiaratchi, C.B., 2013. The influence of coastal reefs on spatial variability in seasonal sand fluxes. Mar. Geol. 344, 132–143.

Gallop, S.L., Kennedy, D.M., Loureiro, C., Naylor, L.A., Muñoz-Pérez, J.J., Jackson, D.W., Fellowes, T.E., 2020. Geologically controlled sandy beaches: their geomorphology, morphodynamics and classification. Sci. Total Environ. 731, 139123.

Harley, M.D., Turner, I.L., Short, A.D., Ranasinghe, R., 2011. Assessment and integration of conventional, RTK-GPS and image-derived beach survey methods for daily to decadal coastal monitoring. Coast. Eng. 58 (2), 194–205.

Harley, M.D., Turner, I.L., Kinsela, M.A., Middleton, J.H., Mumford, P.J., Splinter, K.D., Short, A.D., 2017. Extreme coastal erosion enhanced by anomalous extratropical storm wave direction. Sci. Rep. 7 (1), 1–9.

Hernandez-Pacheco, A., Valls, M.C., 1982. The historic eruptions of La Palma island (Canaries). Arquipélago. Série Ciências da Natureza 3, 83–94.

Himmelstoss, E.A., Henderson, R.E., Kratzmann, M.G., Farris, A.S., 2018. Digital Shoreline Analysis System (DSAS) Version 5.0 User Guide: U.S. Geological Survey Open-File Report 2018–1179 (110 p.).

Hoernle, K.A.J., Carracedo, J.C., 2009. Canary Islands Geology. University of California Press.

Isshiki, N., 1964. Mode of eruption of Miyake-jima volcano in historic times. Bull. Volcanol. 27, 29–48.

Jackson, D.W.T., Cooper, J.A.G., Del Rio, L., 2005. Geological control of beach morphodynamic state. Mar. Geol. 216 (4), 297–314.

Kauahikaua, J., Sherrod, D.R., Cashman, K.V., Heliker, C., 2003. Hawaiian lava-flow dynamics during the Pu'u'O'ō-ō'ō-Kūpaianaha eruption: a tale of two decades. US Geol. Surv. Prof. Pap. 1676, 63.

Klügel, A., Schmincke, H.U., White, J.D.L., Hoernle, K.A., 1999. Chronology and volcanology of the 1949 multi-vent rift-zone eruption on La Palma (Canary Islands). J. Volcanol. Geotherm. Res. 94 (1–4), 267–282.

Langenheim, V.A., Clague, D.A., 1987. The Hawaiian-Emperor Volcanic Chain, Part 2. Hawaiian Volcano Observatory, pp. 55–84.

Lipman, P.W., Moore, J.G., 1996. Mauna Loa lava accumulation rates at the Hilo drill site: Formation of lava deltas during a period of declining overall volcanic growth. J. Geophys. Res. Solid Earth 101 (B5), 11631–11641.

Marrero-Rodríguez, N., Garcia-Romero, L., Sánchez-García, M.J., Hernandez-Calvento, L., Espino, E.P.C., 2020. An historical ecological assessment of land-use evolution and observed landscape change in an arid aeolian sedimentary system. Sci. Total Environ. 716, 137087.

Marrero-Rodríguez, N., Casamayor, M., Sánchez-García, M.J., Alonso, I., 2021. Can long-term beach erosion be solved with soft management measures? Case study of the protected Jandía beaches. Ocean Coast. Manag. 214, 105946.

Mattox, T.N., Mangan, M.T., 1997. Littoral hydrovolcanic explosions: a case study of lava–seawater interaction at Kilauea Volcano. J. Volcanol. Geotherm. Res. 75 (1–2), 1–17.

Mattox, T.N., Heliker, C., Kauahikaua, J., Hon, K., 1993. Development of the 1990 Kalapana flow field, Kilauea volcano, Hawaii. Bull. Volcanol. 55, 407–413.

Mitchell, N.C., Beier, C., Rosin, P.L., Quartau, R., Tempera, F., 2008. Lava penetrating water: submarine lava flows around the coasts of Pico Island, Azores. Geochem. Geophys. Geosyst. 9 (3).

Moore, J.G., Phillips, R.L., Grigg, R.W., Peterson, D.W., Swanson, D.A., 1973. Flow of lava into the sea, 1969–1971, Kilauea Volcano, Hawaii. Geol. Soc. Am. Bull. 84 (2), 537–546.

Muñoz-Pérez, J.J., Tejedor, L., Medina, R., 1999. Equilibrium beach profile model for reef-protected beaches. J. Coast. Res. 950–957.

Phillips, M.R., 2008a. Beach erosion and marine aggregate dredging: a question of evidence. Geogr. J. 174 (4), 332–343.

Phillips, M.R., 2008b. Consequences of short-term changes in coastal processes: a case study. Earth Surf. Proc. Land.: J. Brit. Geomorphol. Res. Group 33 (13), 2094–2107.

Ramalho, R.S., Quartau, R., Trenhaile, A.S., Mitchell, N.C., Woodroffe, C.D., Ávila, S.P., 2013. Coastal evolution on volcanic oceanic islands: a complex interplay between volcanism, erosion, sedimentation, sea-level change and biogenic production. Earth Sci. Rev. 127, 140–170.

Rodriguez-Gonzalez, A., Fernandez-Turiel, J.L., Aulinas, M., Cabrera, M.C., Prieto-Torrell, C., Rodriguez, G.A., Perez-Torrado, F.J., 2022. Lava deltas, a key landform in oceanic volcanic islands: El Hierro, Canary Islands. Geomorphology 416, 108427.

Rodríguez-Padilla, I., Castelle, B., Marieu, V., Morichon, D., 2022. Video-based nearshore bathymetric inversion on a geologically constrained mesotidal beach during storm events. Remote Sens. 14 (16), 3850.

Romero Ruiz, C., 1991. Las manifestaciones volcánicas históricas del Archipiélago Canario (PhD thesis). Univ. of La Laguna, Tenerife, Spain (695 pp.).

Saengsupavanich, C., Seenprachawong, U., Gallardo, W.G., Shivakoti, G.P., 2008. Port-induced erosion prediction and valuation of a local recreational beach. Ecol. Econ. 67 (1), 93–103.

Schmincke, H.U., Sumita, M., 1998. 27. Volcanic evolution of Gran Canaria reconstructed from apron sediments: Synthesis of vicap project drilling. In: Proceedings of the Ocean Drilling Program, Scientific Results, Vol. 157, pp. 443–469.

Siggerud, T.H.O.R., 1972. The volcanic eruption on Jan Mayen 1970. Nor Polarinst Åarb 1970, 5–18.

Skilling, I.P., 2002. Basaltic pahoehoe lava-fed deltas: large-scale characteristics, clast generation, emplacement processes and environmental discrimination. Geol. Soc. Lond., Spec. Publ. 202 (1), 91–113.

Smellie, J.L., Wilch, T.I., Rocchi, S., 2013. 'A 'ā lava-fed deltas: a new reference tool in paleoenvironmental studies. Geology 41 (4), 403–406.

Smith, G.L., Zarillo, G.A., 1990. Calculating long-term shoreline recession rates using aerial photographic and beach profiling techniques. J. Coast. Res. 111–120.

Soule, S.A., Zoeller, M., Parcheta, C., 2022. Submarine lava deltas of the 2018 eruption of Kīlauea volcano. Bull. Volcanol. 83 (4), 23.

Stevenson, J.A., Mitchell, N.C., Mochrie, F., Cassidy, M., Pinkerton, H., 2012. Lava penetrating water: the different behaviours of pāhoehoe and 'a 'ā at the Nesjahraun, Þingvellir, Iceland. Bull. Volcanol. 74, 33–46.

Trenhaile, A., 2016. Rocky coasts—their role as depositional environments. Earth Sci. Rev. 159, 1–13.

Umino, S., Nonaka, M., Kauahikaua, J., 2006. Emplacement of subaerial pahoehoehoe lava sheet flows into water: 1990 Kūpaianaha flow of Kilauea volcano at Kaimū Bay, Hawai'i. Bull. Volcanol. 69, 125–139.

Wilson, J.T., 1963. A possible origin of the Hawaiian Islands. Can. J. Phys. 41 (6), 863–870.